Earth's Future

RESEARCH ARTICLE
10.1029/2024EF005185

Dynamical Factors Heavily Modulate the Future Increase of Sub-Daily Extreme Precipitation in the Alpine-Mediterranean Region

Eleonora Dallan[1,2], Francesco Marra[3], Giorgia Fosser[4], Marco Marani[2,5], and Marco Borga[1,2]

[1]Department of Land Environment Agriculture and Forestry, University of Padova, Padova, Italy, [2]Research Center on Climate Change Impacts, University of Padova, Rovigo, Italy, [3]Department of Geosciences, University of Padova, Padova, Italy, [4]University School for Advanced Studies-IUSS Pavia, Pavia, Italy, [5]Department of Civil, Environmental and Architectural Engineering, University of Padova, Padova, Italy

Abstract Quantifying the future probability of sub-daily extreme precipitation in a changing climate is crucial for risk management, engineering, and insurance. Kilometer-scale convection-permitting climate models (CPMs) represent convective precipitation and complex terrain more realistically than other climate models, thereby enhancing the representation of sub-daily extremes. This study employs a novel statistical approach to evaluate projected changes in extreme sub-daily precipitation and provides a physical interpretation of their driving processes. It focuses on the complex-topography area of northern Italy, where resides almost half of the Italian population and a significant portion of the Italian economy, with a rich diversity in industry, agriculture, tourism. We use precipitation data from a CPMs ensemble covering three periods: historical (1996–2005), near future (2041–2050), far future (2090–2099) under the RCP8.5 scenario. Sub-daily to daily precipitation extremes with return periods up to 100 years are examined. We find a general intensification of extremes across all durations (from 1 to 24 hr), stronger at shorter durations and rarer probabilities. Spatial patterns vary with duration, with higher and significant increases emerging in mountainous areas in Eastern Alps and North Apennines. The detected changes cannot be explained by thermodynamics alone, highlighting the modulating role of the changes in atmospheric dynamics. These findings are crucial for enhancing risk management strategies and adapting to natural hazards in a warming climate. This approach may be exploited in larger scale analysis.

Plain Language Summary This study examines how extreme sub-daily rainfall events are expected to change in the Alpine region and North Italy due to climate change. We use a group of high-resolution climate models and a new statistical approach to provide projections of extreme rainfall for the mid of this century (2041–2050) and the end of this century (2090–2099). Extreme precipitation will generally become more frequent and intense, particularly for shorter durations. The increase is more pronounced in mountainous areas. We find that the larger water vapor content of the atmosphere at higher temperature cannot explain alone the projected changes. Changes in the dynamics of the atmosphere strongly contribute to future extremes. These findings are important for improving risk management practices and adapting for natural hazards in a changing climate, offering insights into how extreme weather patterns may evolve in the future.

Key Points:

- Future changes in sub-daily precipitation extremes are estimated from a novel statistical method and a convection-permitting model ensemble
- Higher increase is projected for shorter durations and higher return periods over the Great Alpine Region
- Changes in the statistical properties of extremes reveal the crucial role of changing atmospheric dynamics

Supporting Information:

Supporting Information may be found in the online version of this article.

Correspondence to:

E. Dallan,
eleonora.dallan@unipd.it

Citation:

Dallan, E., Marra, F., Fosser, G., Marani, M., & Borga, M. (2024). Dynamical factors heavily modulate the future increase of sub-daily extreme precipitation in the alpine-mediterranean region. *Earth's Future*, *12*, e2024EF005185. https://doi.org/10.1029/2024EF005185

Received 30 JUL 2024
Accepted 9 NOV 2024

1. Introduction

Convective processes generate short-duration extreme precipitation events that can trigger various water-related hazards, such as flash floods, urban flooding, and debris flows, resulting in significant damages and casualties. With the expectation of an increased convective activity in a warming climate (e.g., Intergovernmental Panel on Climate Change, 2023), there is a critical need for reliable projections of future short-duration precipitation extremes to guide adaptation strategies.

However, impact assessments have generally used coarse resolution projections from Global Circulation Models (GCMs) and Regional Climate Models (RCMs), which are unable to explicitly resolve atmospheric moist convection and other dynamical processes responsible for extreme precipitation (Orr et al., 2021). During the last two decades, these limitations have been a strong driver in pursuing more advanced, higher resolution climate models, such as Convection Permitting Models (CPM) (Kendon et al., 2017; Prein et al., 2015). Having km-scale resolution, these models can explicitly simulate deep convective systems and provide more realistic

representations of sub-daily precipitation compared to coarser resolution models, in which convection is parameterized (e.g., Prein et al., 2015). These models are able to simulate the effects of both thermodynamic factors (i.e., the rise in saturation water vapor pressure due to temperature increases - Clausius-Clapeyron equation) and dynamical factors, such as shifts in storm tracks and enhanced convergence (Fowler, Ali, et al., 2021). Given these capabilities, they can better capture the probability distribution of precipitation intensity and its spatial distribution, especially in complex terrain (e.g., Fosser et al., 2015), and they promise less uncertainty in extreme precipitation projections than regional models (Fosser et al., 2020, 2024, analyzing CPMs under the CORDEX Flagship Pilot Study on Convective Phenomena). Previous studies have primarily focused on standard percentiles, for example, the 99th or 99.9th percentile of the rainfall intensity in a model run, to evaluate the performance of CPM outputs (e.g., Ban et al., 2014; Pichelli et al., 2021). However, applications for adaptation measures require estimates of rare events corresponding to low, and potentially unobserved, probabilities of occurrence. Hence, to allow the full fruition of the CPMs advantages, a statistical/engineering approach must be adopted instead of those typically used in climate studies. This step forward, however, has been until recently hindered by the limited length of CPM simulations. In fact, the high computational costs associated with CPM simulations restrict the length of simulated periods typically to 10–20 years, which cannot be used by traditional extreme value analyses to infer extreme precipitation associated with the high average recurrence intervals (low probabilities of occurrence).

To address these challenges, Dallan et al. (2023, 2024) used a statistical approach based on the Metastatistical Extreme Value Distribution (MEVD, Marani & Ignaccolo, 2015; Zorzetto et al., 2016; Zorzetto & Marani, 2019, 2020; Marani & Zorzetto, 2019) through a simplified formulation (SMEV, Marra et al., 2019, 2020). Unlike traditional extreme value theory, which focuses on maximum yearly values or exceedances over a high threshold, these methods analyze all the independent realizations of the process, for example, precipitation. In past studies focusing on observational data sets, these methods have demonstrated benefits in reducing uncertainty in estimating extreme precipitation distribution, particularly when working with short data records (e.g., Zorzetto et al., 2016). Thanks to the separation of intensity distribution and yearly occurrence of events in their formulation, these methods have also showed potential in linking statistical findings to underlying physical processes (e.g., Hosseini et al., 2020; Miniussi, Marani, & G Villarini, 2020,Miniussi, Villarini, & Marani, 2020; Formetta et al., 2022; Amponsah et al., 2022; Dallan et al., 2022, 2024). Changes in extreme precipitation are influenced by both thermodynamic and dynamic factors. Thermodynamic factors, describing increased saturation vapor pressure due to temperature rises, and dynamic factors, such as shifts in storm tracks and atmospheric configurations, play a key role (Fowler, Ali, et al., 2021; Trenberth et al., 2003). Variations in the events distributions may be attributed to these processes, as suggested by Dallan et al. (2024). In its first application to projections from a CPM, SMEV showed lower estimation uncertainty than a traditional extreme value approach, especially for precipitation estimates with low exceedance probability, and allowed to attempt a physical interpretation of the results. However, while that study assessed the performance of the methodology, its main limitations are represented by the use of a single CPM. Exploiting a multi-model ensemble is crucial for a more reliable assessment of the projected changes (Kendon et al., 2023).

In this study, for the first time we apply the SMEV approach to 10-year CPM ensemble covering the Alps and northern Italy. Detecting changes in precipitation in this rough orography context is challenging due to the inherent intermittence and variability of precipitation processes, its dependence on large-scale climate variability, and the spatial heterogeneity related to the complex topography. Our objectives are twofold: (a) to quantify projected changes in extreme precipitation from sub-daily to daily precipitation; and (b) to understand the physical mechanisms driving the changes in the statistical characteristics of extreme precipitation and thus in the extreme precipitation itself. By addressing these goals, our aim is to advance understanding of future trends in extreme precipitation and provide enhanced information for adaptation strategies in regions, like mountains, vulnerable to extreme weather events.

2. Materials and Methods

2.1. Study Area

Our analysis focuses on a spatial domain encompassing the Alps, the Po Valley, and the northern part of the Apennines (Figure 1). The relatively high population density and steep slopes make these areas particularly susceptible to natural hazards such as floods and landslides, which are strongly influenced by meteorological

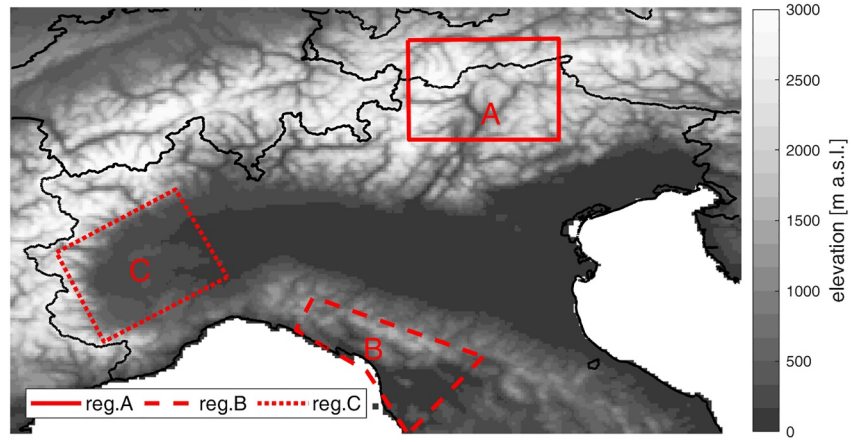

Figure 1. Study area topography, based on one of the CPM models (ETH COSMO-crCLIM). The red lines delimit the three areas for the focus regions analysis: region A (solid line), region B (dashed line), region C (dotted line).

conditions (e.g., Müller et al., 2024; Raymond et al., 2020). This area of about 140,000 km^2 represents about 50% Italian population (~30 million people) and a significant portion of its economy, with a rich diversity in industry, agriculture, tourism.

There is extensive scientific evidence indicating that significant atmospheric warming has occurred and is projected to continue in the study area due to anthropogenic forcing (Hock et al., 2019; Pepin et al., 2015). This warming is estimated at 1.2°C per century over the 20th century (Auer et al., 2007), which is twice the global rate (Brunetti et al., 2009; Gobiet et al., 2014). This trend has intensified in recent decades, with warming rates exceeding 0.3°C per decade (Rottler et al., 2019). Detecting changes in precipitation is more challenging due to the difficulty in observing and simulating this variable in mountainous areas, its dependence on large-scale climate variability, the spatial heterogeneity related to the complex topography, and the inherent intermittence and variability of precipitation processes.

In the following, we will also examine three focus regions (shown in Figure 1) in which past changes in extremes were found to be significant (Libertino et al., 2019), and in which extremes are linked to different large-scale drivers (see the typical patterns of vertically integrated moisture flux in Avanzi et al., 2015 and in Müller et al., 2024), and in which we report significant changes in the projected extremes. These regions will be indicated as: Region A, a mountainous area in the Eastern Alps (size is about 13,000 km^2), subject to westerly weather systems as well as systems coming from the Adriatic Sea, with 50 years return levels ranging from 25 mm (1 hr duration) to 95 mm (24 hr duration); Region B, located between the northern Apennines and the Tyrrhenian Sea (about 10,000 km^2), where the prevalent weather systems from the Tyrrhenian Sea are subject to strong orographic lifting, with 50 years return levels ranging from 65 mm (1 hr duration) to 265 mm (24 hr duration); and Region C, located in the western part of the domain, in a low elevation area which is often shielded from incoming weather by the western Alps (about 13,000 km^2), with 50 years return levels ranging from 48 mm (1 hr duration) to 143 mm (24 hr duration).

2.2. Convection-Permitting Climate Models

We utilize nine CPMs produced under the CORDEX Flagship Pilot Study on Convective Phenomena over Europe and the Mediterranean (FPS Convection; Coppola et al., 2020; Fosser et al., 2024). The CORDEX objective is to understand regional climate and its future changes through a set of coordinated experiments. All CPMs cover the greater Alpine region, as defined by FPS Convection protocol (see Figure 1 in Coppola et al., 2020), use an intermediate nest spanning Europe, and provides hourly data for three 10-year periods: 1996–2005 (historical period), 2041–2050 (near future), and 2090–2099 (far future). To note that MOHC is the only one nesting directly in a high-resolution global model at 25 km and covering slightly different time-slices, that is, 1998–2007 (historical period), 2040–2049 (near future), and 2096–2105 (far future). All future periods are simulated under the Representative Concentration Pathway (RCP) 8.5 scenario. Pichelli et al. (2021) provide an assessment of the biases of the multi-model ensemble during the control period for the Italian part of the study area. The biases

Table 1
List of CPM Models in the Ensemble, With Information on the Institute, the CPM Model, the Driving RCM and GCM Models, and the Original Horizontal Resolution

Institute	CPM *Resolution (km)*	RCM *Resolution (km)*	GCM
CMCC Euro-Mediterranean Center on Climate Change	CCLM5 (Rockel et al., 2008; Adinolfi et al., 2021) *3 km*	CCLM5 (Rockel et al., 2008; Adinolfi et al., 2021) *12 km*	EC-Earth
KIT Karlsruhe Institute of Technology	CCLM5 (Rockel et al., 2008; Sørland et al., 2021; Baldauf et al., 2011) *3 km*	CCLM4 (Sørland et al., 2021; Keuler et al., 2016) *12 km*	MPI-ESM-LR
ETH Institute for Atmospheric and Climate Science	COSMO-crCLIM (Rockel et al., 2008; Leutwyler et al., 2016) *2.2 km*	COSMO-crCLIM (Rockel et al., 2008; Leutwyler et al., 2017) *12 km*	MPI-ESM-LR
CNRM Center National de Recherches Météorologiques	CNRM-AROME41t1 (Caillaud et al., 2021) *2.5 km*	CNRM-ALADIN63 (Nabat et al., 2020) *12 km*	CNRM-CM5
DMI-MET-SMHI DMI-MET Norway- SMHI HARMONIE-Climate community	HCLIM38-AROME (Belušić et al., 2020) *3 km*	HCLIM38-ALADIN (Belušić et al., 2020) *12 km*	EC-Earth
KNMI The Royal Netherlands Meteorological Institute	HCLIM38-AROME (Belušić et al., 2020) *2.5 km*	RACMO2.3 (Noël et al., 2015) *12 km*	EC-Earth
FZJ-IBG3 and IDL Research Center Julich and Institute Dom Luiz	WRF3.8.1CA (Powers et al., 2017) *3 km*	WRF3.8.1CA (Powers et al., 2017) *12 km*	EC-Earth
ICTP Abdus Salam Internatinal Center for Theoretical and Earth System Physics	RegCM4 (Coppola et al., 2021) *3 km*	RegCM4 (Coppola et al., 2021) *12 km*	HadGEM
MOHC Met Office Hadley Center Exeter	HadREM_UM10.1 (Berthou et al., 2020; Chan et al., 2020) *2.2 km*		HadGEM (25 km, atmosphere-only)

computed for the 99.9th percentile over the wet periods, range between 15% at 1 hr and 1.5% at 24 hr for the fall season, and between 8.3% at 1 hr and 3.9% at 24 hr for the summer season.

Table 1 outlines the nine models used in this study, along with the corresponding institutions and original spatial resolutions. For the near future period, the ensemble consists of eight models, excluding the WRF3.8.1CA model for which we had no data. A conservative remapping to a common 3-km grid is applied to all simulations before conducting statistical analyses, resulting in approximately 45,000 grid points in the study area for each model.

2.3. Estimation of Extreme Return Levels

In this study, we use the Simplified Metastatistical Extreme Value (SMEV, Marra et al., 2019, 2020) framework to estimate extreme return levels. SMEV is a simplified form of the Metastatistical Extreme Value (Marani & Ignaccolo, 2015) in which inter-annual variability is neglected (Marra et al., 2019). These non-asymptotic approaches rely on specifying the tail behavior of the distribution $F(x)$ of the parent process x and considering the finite number n of occurrences in a year, instead of taking the asymptotic limit $n \rightarrow \infty$ of the extreme value theorem. Said x the duration maxima of independent storms at a given temporal aggregation, here 1, 3, 6, 12, or 24 hr, the cumulative distribution function of the annual maxima can be approximated as:

$$G_{SMEV}(x) \simeq F(x)^n \quad (1)$$

where n is the average number of ordinary events per year. In the case of precipitation, $F(x)$ is often assumed to be a two-parameter Weibull distribution (Marani & Ignaccolo, 2015), as justified by atmospheric dynamics reasoning (Wilson & Toumi, 2005). This assumption well describes observations (e.g., Marra et al., 2023; Zorzetto et al., 2016), and is supported by stochastic modeling results (Papalexiou, 2022). The two-parameter Weibull distribution is defined as:

$$F(x) = 1 - exp\left(-\left(\frac{x}{\lambda}\right)^{\kappa}\right) \quad (2)$$

In the following, we will discuss the results in terms of the values of the Weibull parameters. The first parameter, λ, is a scale parameter that rescales all the values of the distribution by a common factor. The shape parameter, κ, is a measure of how quickly the exceedance probability of large events decreases with their magnitude. It will be referred to as a measure of tail "heaviness". A value $\kappa > 1$ is associated with lighter tails in which the probability of large events decreases more rapidly than the exponential case. Values $\kappa < 1$ are associated with heavier tails, in which the exceedance probability of large events decreases more slowly than the exponential case.

Independent storms are identified as wet periods separated by dry hiatuses of at least 24 hr (<0.1 mm reported in 24 consecutive hourly intervals; e.g. Dallan et al., 2024). Ordinary events are then defined as the peak intensities recorded in each storm, for the duration of interest. The empirical tail of the recorded ordinary-event data set that can be approximated with a Weibull distribution is identified using a properly defined left-censoring threshold (Marra et al., 2020). Following Dallan et al. (2023, 2024), who applied the SMEV approach on simulations from a CPM in the same region, we identify a suitable threshold using the test by Marra et al. (2023). The 90th percentile of the ordinary events is used as the left-censoring threshold for hourly duration, and the 85th percentile for longer durations. Under this framework, any threshold higher than the selected one provides virtually indistinguishable results, aside from estimation noises for excessively high thresholds. The sensitivity to these specific choices is thus negligible (Marra et al., 2023). For each simulated time period, we estimate return levels up to 1% annual exceedance probability (100 years return period) for durations of 1, 3, 6, 12, 24 hr at each grid point, from the nine CPMs.

2.4. Future Change and Its Significance

We evaluate the projected changes in return levels and distribution parameters for both near-future and far-future simulations compared to the historical period across all grid points within the study region. For each model i, on each grid point j, the future relative change $C_{X,ij}$ is calculated as the percentage difference between future (near or far) and historical value of variable X, and expressed as:

$$C_{X,ij}[\%] = \frac{X_{fut,ij} - X_{his,ij}}{X_{his,ij}} \cdot 100 \quad (3)$$

The projected change for the ensemble $C_{X,i}$ [%] is then computed as the median of the M-ensemble-member change, in each grid point i:

$$C_{X,i} = median(C_{X,ij}) \quad j = 1,..,M \quad (4)$$

We thus obtain the spatial description of the projected ensemble-median change in the study area. The variables X considered for the computation of future changes are: mean annual maxima in the 10 years period, return levels up to 100 years, parameters of the distribution, yearly number of storms.

In each grid point, we consider two important aspects: the model agreement and the significance of the changes. The models agree if more than 60% of ensemble members (i.e., 5 out of 8 for the near future and 6 out of 9 for the far future) show the same direction of change (either positive or negative), otherwise the grid point is labeled as "non-concordant". In the results section, we show in the maps the location and the fraction of non-concordant points.

10.1029/2024EF005185

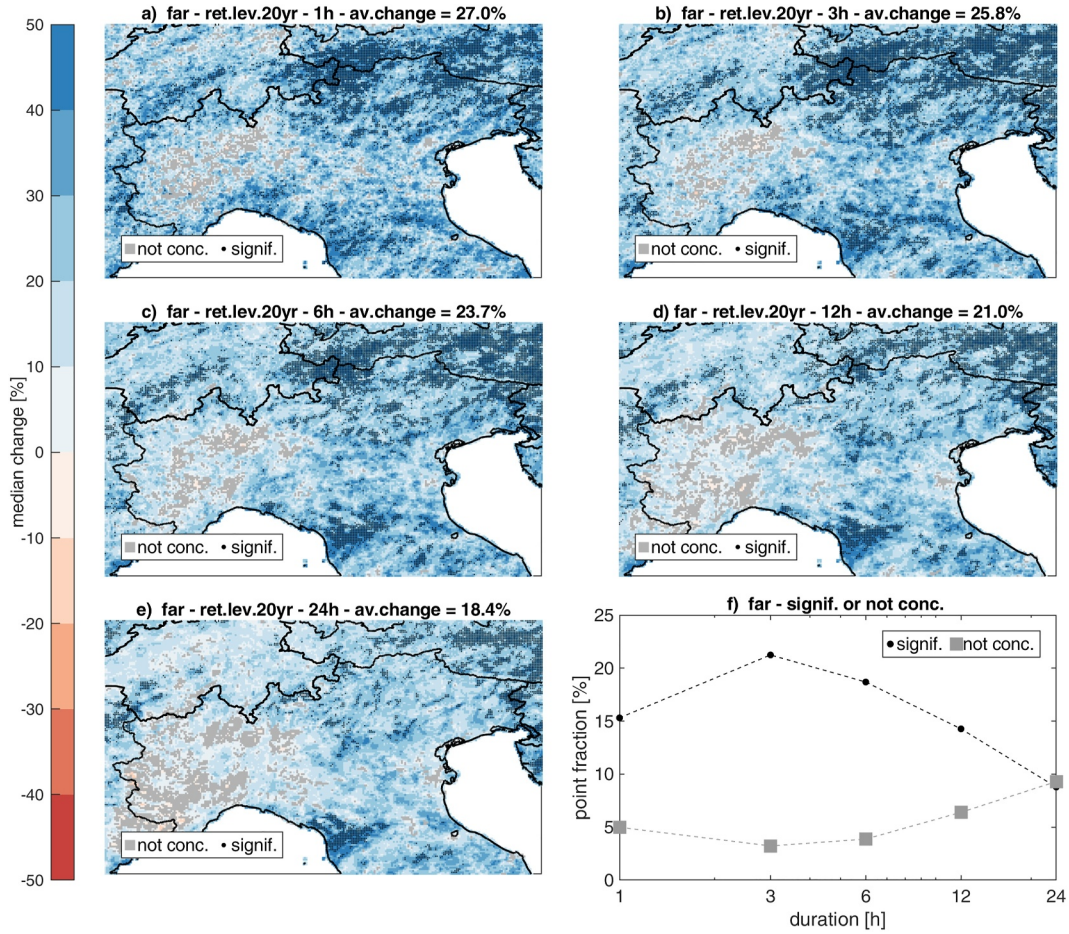

Figure 2. Far future change for the 20 years return level. Panels a to e: ensemble-median change at 1-3-6-12-24 hr durations (blue to red color scale); average value in the area is indicated in the panel title; gray grid cells indicate no concordance in the ensemble members; black dots indicate significant change at 5% significance level. Panel f: fraction of significant (black line) and no concordant (gray line) points in the domain for the 5 durations.

For each ensemble member, the statistical significance of the estimated changes at each grid point is assessed at the 5% significance level using a permutation test with 1,000 permutations between historical and future periods, following the method proposed by Dallan et al. (2024). Thus, grid points where the change is concordant and is significant for more than 50% of the ensemble members are labeled as "significant points".

3. Results

The Results section presents first the spatial description and summary statistics of the changes across the entire domain for a "moderate" precipitation extreme, such as the 20 years return level (in Section 3.1), and for a rarer extreme that is often a reference for hydrological design, the 100 years return level (Section 3.2) (the Figures S1 and S2 in Supporting Information S1 related to the near future). For the far future change, also results for the change in the mean annual maxima and parameters are reported in the supplementary material (Figures S3–S6 in Supporting Information S1). We then describe the relation of significant changes in extreme rainfall with duration and with extremeness, and the change in the parameters of their distribution (Section 3.3). Finally, we analyze the changes in the three focus regions A, B, C, where different behaviors emerge in the present study as in previous studies (Section 3.4).

Given the moderate change found in the near future, with no appreciable statistical significance, we focus here on results for the far future. We provide just a short description of the main results for the near future, while all the related figures are provided in Supporting Information S1.

3.1. Future Change in the 20 Years Return Levels

The maps of the ensemble-median future change in the 20 years return levels are reported in Figure 2 for the far future and in the supplemental material Figure S1 in Supporting Information S1 for the near future. Blue (red) colors indicate an increase (decrease) in return levels according to the majority of the models ("concordant" points, where 5 models out of 8 for near future, 6 models out of 9 for the far future). In gray color, grid cells in which no agreement in the direction of change is observed (non-concordant points). Black dots indicate grid cells in which the change is statistically significant (5% level, based on the permutation test) in the majority of the models. The average projected change in the entire domain is reported in the panel title.

In the far future, the maps show a higher positive change than in the near future, with an average across the domain that ranges from 27% at 1h to 18% at 24hr (Figure 2, panels a to e). The increase is higher in the northeastern quadrant, with the higher values, exceeding 40%, at ≤6 hr durations. In the northwestern Alps the change is also positive but slightly lower (20%–30%). A positive change above 40% emerges at durations ≥3h in the southern part of the domain, between the western coastline and northern Apennines mountains. A non-significant increase characterizes the central and eastern lowland of the Po river valley, while no concordant changes (about 5%–10% of points in the domain, Figure 2f) are located in a western region corresponding to a lowland area surrounded by mountains (see Figure 1). The fraction of significant points in the study area varies from 10% to 20% (Figure 2f), higher at 3 hr duration. They are mostly located in the central and eastern Alps at durations ≤6h and in the southwestern region at durations ≥3h. In the near future, most of the domain shows positive changes in the return levels, with an average change over the area around 10%–11% for all the durations (Figures S1a–S1e in Supporting Information S1) and slightly higher increase in the Eastern Alps. No concordant change (about 10%–15% of points in the area, as shown in Figure S1f in Supporting Information S1) appears in the western and central part of the domain. The low fraction of significant points in the study area (1%–2%, Figure S1f in Supporting Information S1) is below the 5% significance level and can't be considered as a robust signal.

3.2. Future Change in the 100 Years Return Levels

In the far future, the increase in the 100 years return level is higher than for the 20 years return level, with an average change in the domain from about 30% at 1h to 21% at 24hr (Figure 3, panels a to e). At ≤6 hr durations, the increase is higher in the northeastern quadrant, with values above 40%, and in the northwestern Alps, about 30%. A positive change above 40% emerges at durations ≥3h in the southwestern part of the domain, as seen for the 20 years return level. Non-significant increases characterize the central and eastern lowland of the Po river valley, and no concordant changes (about 5%–10% of points in the domain, Figure 3f) are present in the western lowland region. The fraction of significant points in the study area varies from about 8% to 18% (Figure 3f), slightly lower than for the 20 years return period. Significant changes are mostly located in the central and eastern Alps at durations ≤3h and in the southwestern region at durations ≥3h. In the near future, the average change in the 100 years return level is similar to the 20 years return level change (11%–12% for all the durations, Figure S2 in Supporting Information S1, panels a to e), with non-concordant change in the western and central part of the domain. The fraction points in which the changes are deemed as statistically significant (1%–2%, Figure S2f in Supporting Information S1) is very low.

3.3. Significant Changes on Extremes and Their Distribution Parameters

For the "significant points" (Section 2.4), we analyze the dependence of the changes with durations and their relation with the change in the parameters of the distribution. The "average significant change" is calculated as the average of the ensemble-median change only on the significant points; for the parameters scale and shape and yearly number of events n, their average change is calculated based on the significant points at 20 years return level. The average significant change is reported in Figure 4 for the far future period, while the analysis is not done for the near future, where just 1%–2% of points in the domain are significant.

To represent different levels of extreme precipitation severity, we show here the results for the mean annual maximum (AM) in the 10 years, the 20 years return levels and the 100 years return levels. There is generally higher positive change at hourly duration than at 24 hr: from 1 to 24 hr, the change is ranging about from 32% to 28% for AM, from 43% to 34% for 20 years return level, from 51% to 40% for 100 years return level. The difference between short and long durations is enhanced for rarer events (higher return period). The positive change

10.1029/2024EF005185

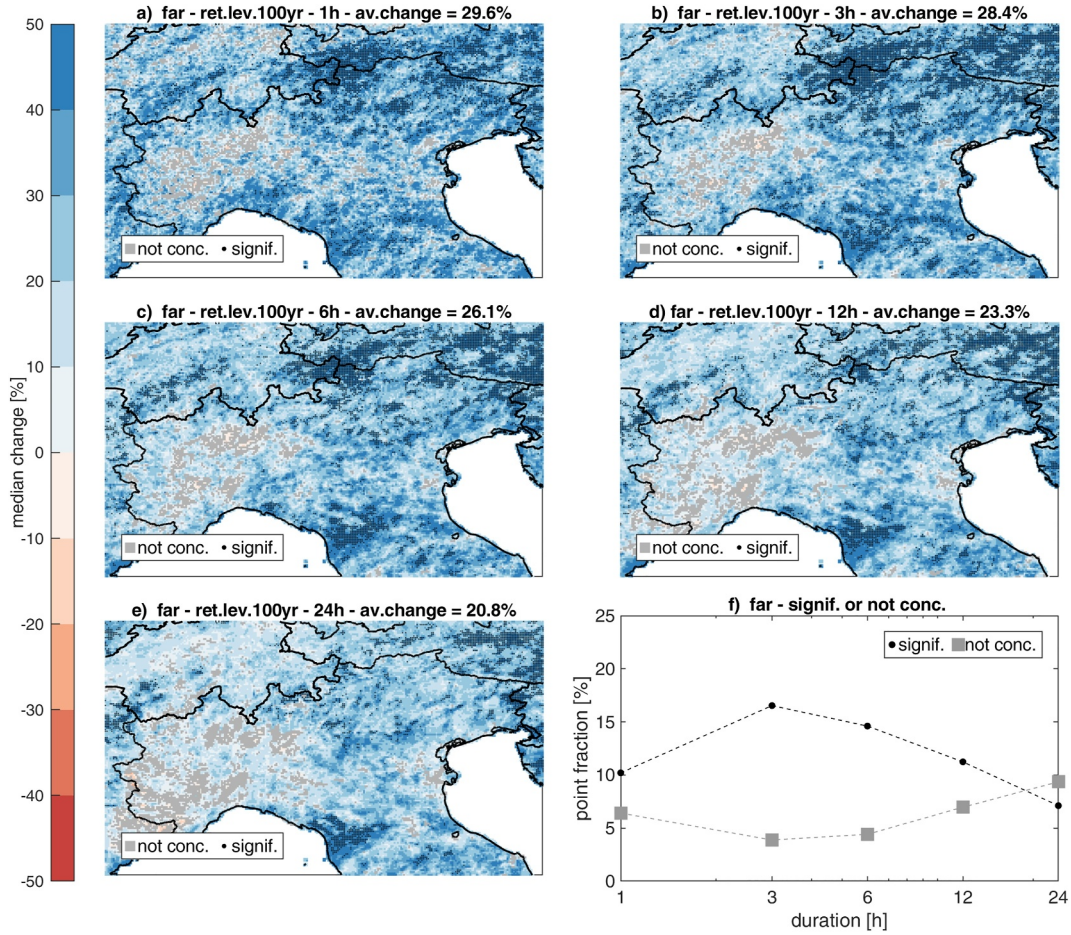

Figure 3. Same as Figure 2, for the 100 years return level.

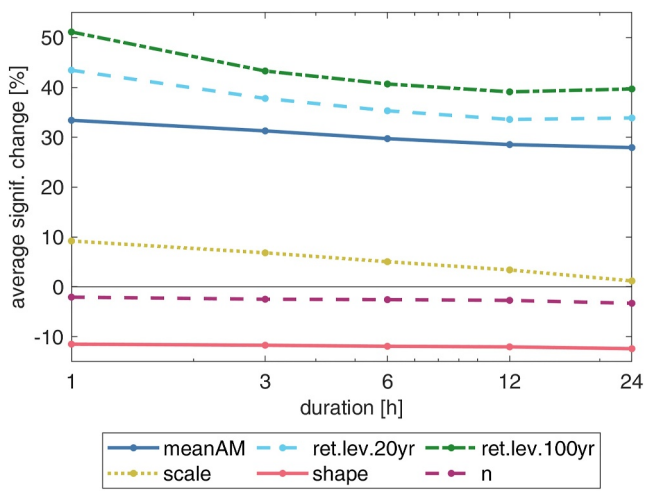

Figure 4. Average on significant points of the ensemble-median change in the far future, at different durations. For extreme rainfall quantities (i.e., mean annual maximum in the 10, 20 years return level and 100 years return level) the average is calculated based on their significant points; for the parameters scale and shape and for the yearly number of events the average is calculated based on the significant point at 20 years return level.

is always higher with higher severity of precipitation, that is passing from mean AM to 20–100 years return level. Indeed, we find a monotonic increase for the future change in return level, of about 45%–50% from 2 to 100 years return time (not shown for the sake of brevity).

We also computed single-model average percent change in extreme precipitation for the various durations and for the different return period (Figure S7 in Supporting Information S1). The results show a marked decrease in the spread among the models from 1 hour (with changes ranging from ∼25% to 80% at 20 years return period and from 30% to 115% at 100 years return period) to 24 hr (with changes ranging from 20% to ∼45% at 20 years return period and from 20% to 50% at 100 years return period).

The scale parameter shows a positive change of about 10% at 1 hr, monotonically decreasing with increasing durations reaching about 0% at 24 hr. A negative change is found for the shape parameter across all the durations, about −11% at 1 hr and −12% at 24hr. A decrease in the shape implies distribution tails that are becoming heavier in the far future. The average yearly number of events is generally slightly decreasing. The analysis of the changes in parameters allows us to attempt a physical interpretation to the changes found in the extreme precipitation, and this is discussed at Section 4.

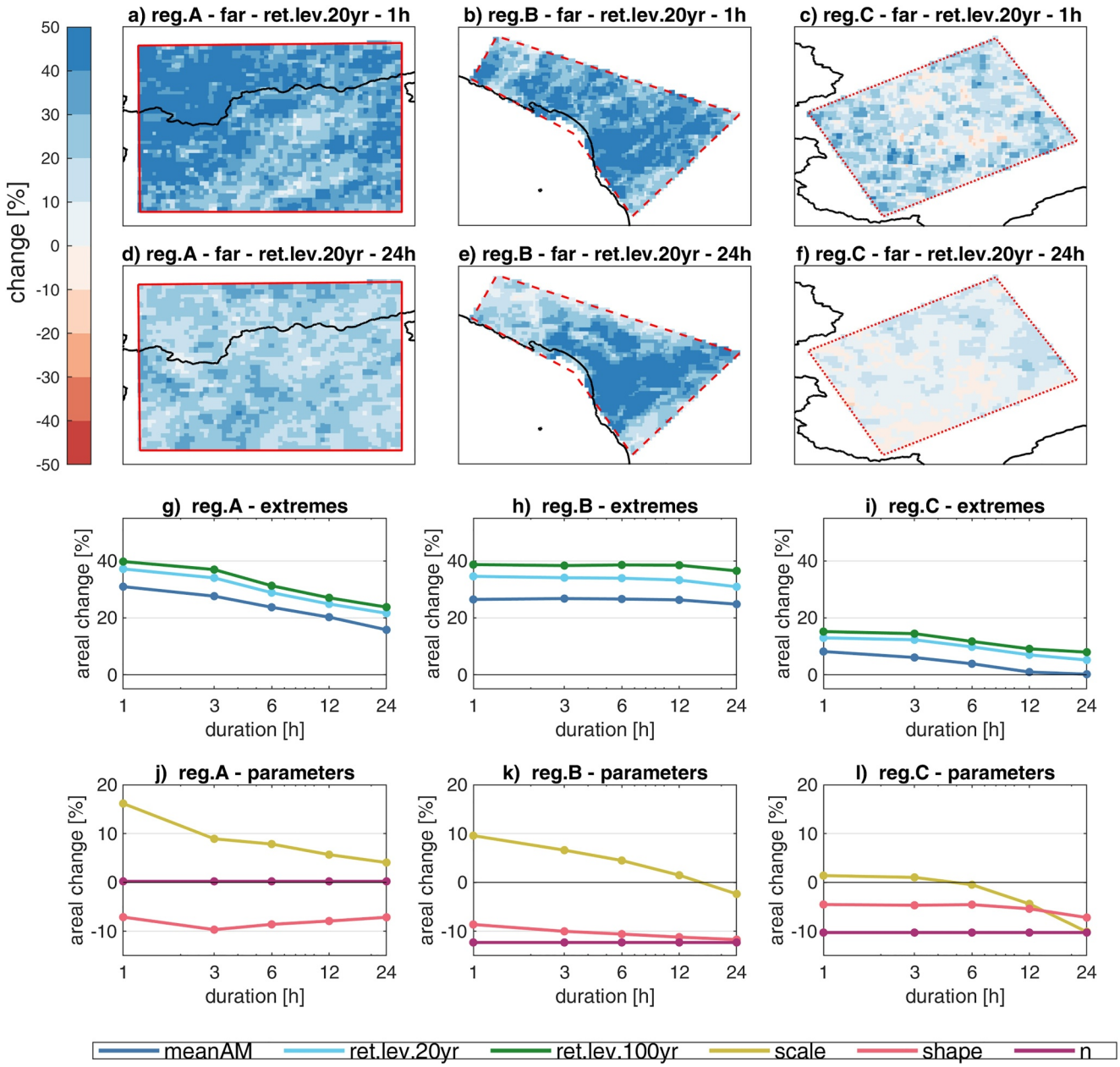

Figure 5. (panels a to f) Maps of the far future changes in 20 years return level in the three focus regions A, B, C, for 1 and 24 hr (panels g-h-i) Areal average far future change in the three focus regions for extreme precipitation for all the durations: mean annual maxima, 20 years return level, 100 years return level (panels j-k-l) Areal average far future change in the three focus regions for the parameters scale and shape and yearly number of events for all the durations.

3.4. Future Changes in Different Focus Regions

Future changes are here analyzed for the three focus regions A, B, C (as reported in Figure 1). In the present study, we also observe a homogeneous pattern of change within each of these regions, which is, however, different among the three regions. By isolating them we can explore and highlight if and how different future changes in rainfall extremes can occur in different regions. We analyze here the far future (Figure 5), while for the near future see Figure S3 in Supporting Information S1. Areal averages are computed among all grid points in each region. Fraction of significant points for the 20 years return level at 1 hr (24 hr) is ~50% (10%) in region A, 16% (24%) in region B, ~0% in region C.

Regions A and B exhibit an average change that is quite similar in magnitude (35%–40%) at 1–3 hr duration (Figures 5g and 5h), uniform and internally concordant (Figures 5a and 5b; negligible fraction of not concordant points in both regions). For the 20 years return level, changes in region A show a strong relation with duration, decreasing from about a 37% change at 1 hr to about 20% change at 24 hr (Figure 5g), while Region B exhibits an almost constant spatially averaged change across durations (about 30%–35%, Figure 5h). Region C experiences a much lower change than the other regions, from about 12% at 1h duration to about 5% at 24 hr. The low spatially averaged values are due to a combination of low magnitude changes and to the presence of both positive and negative changes (fraction of not concordant points is 32% at 1h duration and −50% at 24 hr). For all the focus regions, the change is higher for rarer events (100 years return level). In the near future (Figure S8 in Supporting Information S1, panels a–i), all regions show lower change for extremes than in the far future (about 15%–20% Region A, 10%–15% in Region B, <10% in Region C), almost constant across durations. Also in the near future, higher change is found for higher return period.

The average changes in the parameters of the distribution and number of events are presented in Figure 5 panels *j*, k, *l* (near future in Figure S8 in Supporting Information S1 panels *j*, k, l). In region A scale has a positive change in both future periods, higher in the far future, and decreasing with increasing duration (from about 15% at 1%–5% at 24 hr in far future). The negative change in the shape parameter describes a projected increase in the distribution tail heaviness, more in the far future than in the near future. Its change is enhanced at 3 hr duration, while slightly diminishing at longer durations. No change is projected in the yearly number of events. In general, in region A the tendency of change in the parameters in the near future seems in some way enhanced in the far future (scale increasing more, shape decreasing more). In region B, the scale parameter in the far future has the higher positive change at 1 hr (10%) and decreases till reaching a low negative value at 24hr (low positive change of about 5%–6% at all durations is found in the near future). The distribution tail is projected to be much heavier in the far future and at longer duration (scale change of about −12%). Also, the number of events strongly decreases in the far future (−12% vs. −4% in the near future). Finally, in region C the scale parameter shows a slightly positive change only at 1h, changes being negative, with values up to −10%, in the far future at 24 hr. The change in the shape parameter is negative (about −5%) in the far future, confirming the tendency of increasing tail heaviness as found in the other regions, even if here it is less enhanced. Yearly number of events is projected to decrease, with a more marked signal in the far future (−10%).

4. Discussion

4.1. Projected Changes in Return Levels

The results on future change in return levels show a general increase in the study area, which is enhanced in the far future with respect to the near future. Shorter durations (1–3 hr) and longer return periods (100 years) exhibit the highest increases, up to almost 50% in the ensemble-median value for some points. For the far future, the significant changes emerge prominently in two mountainous areas: the central-eastern Alps up to 6 hr, and the southwestern side of the north Apennines from 3 hr. The peak in the significance percentage at 3 hr in Figures 2f and 3f can be related to the lower statistical significance at 1h duration, for which SMEV is applied on 10% upper tail of ordinary events, in contrast with the 15% used for all the other durations.

The consistency in the spatial pattern of change, and the similar fraction of significant points between the 20 and 100 years return levels indicate that the climate change signal is not masked by the estimates' uncertainty also for the higher return period considered. As previously shown in Dallan et al., 2024, the proposed methodology for estimating future changes in extreme precipitation can be considered to be effective even when applied to short CPM runs. Moreover, the use of a multi-model ensemble attenuates the partial masking of climate change signal by natural variability, which is dominant source of uncertainty at convection-permitting scale especially for short-durations (Fosser et al., 2024). In fact, each projection is the sum of a smooth forced signal and the accompanying natural variability noise, different and not in phase (including on multi-decadal timescales) among models. Combining models allows the climate change signal to emerge more clearly by averaging out the "noise" introduced by year-to-year natural variability. Similarly, the multi-model ensemble approach partially removes the limitations due to the use of decadal simulations to sample non-linear future precipitation changes, such as the temporal clustering of record and non-record events (Kendon et al., 2023). Furthermore, a multi-model ensemble enables the evaluation of model uncertainty, which are crucial for informed decision-making and robust adaptation policy.

The dependence on duration of the significant changes in extreme precipitation (Figure 4) shows that, in general, short duration extremes are projected to increase more than the longer duration extremes. This is in line with what generally expected in response to thermodynamic forcing, and follows the general tendency found in Ban et al. (2020), based on a single model, and in Pichelli et al. (2021) for a 12-model ensemble, for averaged areal change in moderate extremes. Ban et al. (2020) found a higher average increase for the 1 hr return levels than for the 24 hr and 5 days durations (average change in the domain in fall season ∼30% at 1h and 20% at 24 hr for 100 years return level), and suggested an increasing contribution of convective events with climate change. Pichelli et al. (2021) found that, in a region similar to our domain, the 99.9th rainfall percentile has higher positive average future change at 1 hr duration (above 40% in regions similar to our region A and C) than at 24 hr, more pronounced in autumn (in summer, 24 hr duration showed a decrease). Marra et al. (2024), with a different approach, reported percent changes up to 38% for 10 years return levels at 10 min rainfall duration. We build on these studies, exploring the entire range of sub-daily durations, evaluating the statistical significance of the projected changes, and, mostly, extrapolating to return levels of interest for practical applications. Our results suggest that, in the study area, convective storms related to short duration intense precipitation are expected to become more severe with climate change at a rate that is higher than the one of weather patterns related to longer duration extremes. In some areas, this trend already emerged in the recent decades (Dallan et al., 2022).

The spatial pattern of change for the return levels can be just partially compared with changes from Pichelli et al., 2021, although the latter were evaluated for the 99.9th rainfall percentile of the entire data series and for separate seasons, and therefore represent relatively low annual exceedance probabilities (the 99.9th seasonal percentile is exceeded on average twice a year). At 1 hr duration, they also found an increase in extreme-value intensity over the Eastern Alps (both in summer and autumn) and in the western-northern Apennines (in autumn). At 24 hr duration, they also found an increase in the eastern Alps (in summer), and relevant increase in the north east Italy and Tuscany (in autumn). This suggests that different physical processes may underlie the changes at different locations, as we discuss in the next section.

The dependence on severity levels emerges by comparing changes in 20 and 100 years return levels from both the areal average statistics and the statistics on significant points. This is minimal in the near future (Figures S1 and S2 in Supporting Information S1), while clearly emerges in the far future. Indeed higher positive change for higher severity level is found across all durations both in the areal average values (Figures 2 and 3) and particularly relevant on significant points (Figure 4). This is partially in line with Ban et al. (2020), showing an averaged future increase just slightly higher for higher return periods, but their evaluations were limited to just one model and summer hourly extremes.

Our findings, based on an ensemble of CPMs and a novel statistical method, allow us to distinguish the magnitude of future changes across different durations and severity levels up to 100 years return period, and to characterize the significance of the change in different locations. This is unprecedented information for risk management. Our results highlight that relevant and significant future increases in extreme rainfall are expected in some complex-terrain areas, which are more vulnerable to rainfall-driven hydro-geological hazards, with important implications for the derivation of future intensity-duration-frequency curves used for hazard assessment (e.g., Martel et al., 2021). However, short duration precipitation and complex-orography area represent the most uncertain conditions in estimation of high return periods. Future work would be required to quantify the uncertainty sources and their variation according to precipitation duration, orography and other geographical features, for example, by the use of bootstrap techniques and approaches such as those considered in Reggiani et al. (2021). We should also recognize the limitations of CPMs. These models are still affected by some biases, such as an overestimation of heavy rainfall due to under-resolved cloud processes (Fowler, Ali, et al., 2021) and lack of capability to capture the small-scale details of storms, which in some cases limit the CPM added value, as shown for instance in Schaaf and Feser (2018).

4.2. Projected Changes in Distribution Parameters and Their Physical Interpretation

The dependence of the changes in extreme precipitation with severity levels (described in Section 4.1) indicates that the distribution tails, governing the relation between high and very-high extremes, are expected to be heavier in the far future than in the near future across all durations. Indeed, this consideration is in line with the negative change of the shape parameter of about −11% found in the far future (Figure 4), a change which is similar across durations. At 1 hr duration, the higher increase with respect to the other durations found in the far future can be

explained by the higher positive change in the scale parameter (10% at 1h and about 0% at 24 hr on significant points). Increasing scale combined with decreasing shape enhances the positive change at 1 hr in the far future.

Changes in extreme precipitation are related to the interplay of thermodynamic and dynamical factors. Thermodynamic factors include the rise in saturation water vapor pressure due to temperature increases (Clausius-Clapeyron equation), while dynamical factors may involve changes in the proportion of atmospheric configurations associated with precipitation, shifts in storm tracks, enhanced convergence, etc (e.g., Trenberth et al., 2003). The ability of our approach to distinguish between the intensity and frequency of storm occurrences allows us to propose a physical interpretation of our results. Changes in the distribution of the ordinary events (in terms of their parameters) can be linked to changes in local-scale atmospheric dynamic and thermodynamic factors, as well as differences in dynamical factors associated with large-scale atmospheric circulation, as proposed by Dallan et al. (2024). In our study, we benefit from using an ensemble of models and a broader area, which enables a more robust and general discussion of the results. Short-duration precipitation extremes are mostly related to convective processes and are more sensitive to and better constrained by thermodynamics, while longer-duration (daily) extremes are related to a wider variety of processes, which often depend on large-scale weather patterns (e.g., Chan et al., 2023; Fowler, Wasko, & Prein, 2021). Nevertheless, thermodynamic considerations are not sufficient to explain our findings even at short durations. If the Clausius-Clapeyron equation was the only factor explaining changes in extreme precipitation, extremes would increase by a common factor irrespective of their severity (exceedance probability, return period). Our results show that this is never the case, with rarer events showing much higher increase than moderate extremes, and that the shape parameter is also projected to change. The decrease we find in the shape parameter is indicative of the important role played by atmospheric dynamics in modulating future changes in precipitation. These dynamic factors may encompass changes in large-scale atmospheric circulation, such as different proportions of synoptic systems leading to precipitation, or changes in large-scale convergence, as well as changes in local dynamics, such as enhanced convergence in convective cells, or enhanced vertical velocities. These results, which are here formalized for the first time based on future projections of extreme return levels as low as 1% annual exceedance probability, are in line with previous results based on observations (Peleg et al., 2018; Wasko et al., 2016) and pseudo-global warming projections (Armon et al., 2022) for other regions of the globe. The higher rise in the scale parameter at short duration than at daily duration may indicate that thermodynamic influences become increasingly evident toward the end of the century. The slight decrease in the yearly number of events n in the far future is also linked with changes in atmospheric circulation. We found (see Figure S6 in Supporting Information S1) a stronger decrease of n in the southern part of the domain, which may be associated with the expected poleward shift in extratropical cyclones track induced by the expansion of the Hadley cell (Lu et al., 2007).

These results provide an unprecedented physical understanding of the projected changes in extreme return levels in a warming climate. They reveal the key role of dynamic factors in modulating the increasing of short duration extremes in our study area. The proposed approach, here applied at a regional scale, could be extended to the evaluation of projected changes in sub-daily precipitation extremes in wider areas or other regions for which ensemble CPM simulations are available, strengthening the physical interpretation here provided at a regional scale.

4.3. Insights From the Analysis of the Focus Regions

The analysis on the focus regions shown at Section 3.4 reveals interesting similarities and differences in the projected changes, discussed here together with a possible physical interpretation of the results.

Region A (north-eastern study domain) shows the highest positive change of extremes at short durations, passing from about 38% at 1 hr to 20% at 24 hr. This can be explained by the combination of an increased scale (16% at 1 hr, 4% at 24 hr) and decreased shape parameter values (−7% at 1 hr, −6% at 24 hr), describing a future enhancement of both the scale of the distribution and its tail heaviness. The decreasing shape parameter, with similar magnitude across durations, suggests a contribution of dynamical processes in modulating extreme events' changes across all durations. The relevant increase of scale at short durations indicates an important effect related to temperature scaling, as expected by thermodynamics considerations. Thus, in region A, the increase in short duration extremes could be related to different atmospheric controls enhancing convection-like events. In the near future (Figure S3 in Supporting Information S1) the tendencies in extremes and parameters are similar to the far

future but weaker, especially at 1 hr, thus suggesting similar controlling factors which further enhance in the far future.

Region B shows a high positive change of extremes which is similar at all durations (about 35% at 1 hr and 30% at 24 hr, Figure 4), with significance emerging at longer durations (Figure 2). Even if the change is similar among durations, it is related to different changes in parameters at different durations. Indeed, at 1h duration, similarly to region A, an increased scale (10%) combines with a decreased shape (−8%). At 24 hr, scale is decreasing while the shape negative change (−12%) indicates much heavier distribution tails as responsible for increasing extremes. The strong negative change in the shape suggests that local and large-scale dynamical factors play a fundamental role in shaping the change in extremes across all durations, and particularly at daily durations. The thermodynamic control related to temperature scaling seems emerging at short duration, but it is less relevant than in region A. The decreasing scale at 24 hr could be indicative of changes in the large-scale forcing in the region. This is also confirmed by a relevant decrease in the average number of storms per year, which suggests a decreasing number of precipitating weather systems reaching the region and by the specific seasonal changes reported by Pichelli et al. (2021).

In region C, the far future maps in Figure 5 show slightly positive to null average change in the extremes. Similarly to region A, changes are higher for shorter durations. The change in the parameters has instead some similarity with region B. Indeed, the scale parameter is (slightly) increasing at 1h and then decreasing at longer duration. The change in the shape parameter is negative (enhancement of the tail heaviness), especially at 24 hr, and it compensates for the decreasing effect on extremes of the decreasing scale. To be noted, the presence of a strong reduction of the number of events, which can be related to large scale dynamics, also confirmed by the seasonal changes reported by Pichelli et al. (2021).

The differences emerging in the three focus regions may be due to differential changes across the different prevailing processes characterizing each region (e.g., see the prominent direction of moisture flux in Avanzi et al., 2015). However, some similarities also emerge. The change in the scale parameter is positive at short duration and decreases with increasing duration, consistently with the expected effect of temperature increase that can be extracted from extreme precipitation-temperature scaling relations. Another similarity is the negative change in the shape parameter, indicating in the three focus regions an expected (different-magnitude) enhancement of tail heaviness (further intensification of rare vs. moderate events) that can be related with dynamical factors.

5. Conclusions

The study analyzes the projected changes in sub-daily extreme precipitation and the parameters of their statistical distribution using an ensemble of CPMs. In the far future (2090–2099), the climate change signal is more relevant than in the near future (2041–2050), with concordant changes among models, and significance emerging in some areas. The whole domain experiences a general increase in extreme precipitation across all durations, showing stronger enhancements at shorter durations (areal average change of about 40% for the 20 years return level at 1h) and higher return periods. Spatial patterns vary by duration, with stronger increases emerging in two complex orography areas (Eastern Alps and west side of Northern Apennines). Changes in distribution parameters reveal increased scale at short durations and increased tail heaviness across all durations, explaining the significant change in short-duration rarer return levels. The analysis on three focus regions allows us to distinguish the diverse physical processes modulating the extreme precipitation changes. In a region A (eastern Alps), the increase, higher at 1 hr and decreasing with increasing durations, seems related to dynamical factors in combination to thermodynamic enhancement at the short duration. In region C (west side of the northern Apennines), there is a relevant increase of extremes at all durations, explained by an important increase in the heaviness of the distribution tail which could be mostly related to enhanced dynamics atmospheric processes.

Our findings underscore the importance of assessing extreme precipitation changes as a function of their yearly probability of occurrence. Notably, the largest projected increase is obtained for short-duration, long-return-period events, with significant implications for hazard assessments. We also found that in the focus regions similar changes can be related to different changes in the statistical properties of the precipitation distributions, in turn related to different underlying physical processes. In our study area, we find that dynamical factors have a fundamental role in modulating the thermodynamic factors on the projected

increase in extremes across all the durations. These findings improve our knowledge of future changes in extremes and their atmospheric drivers and can be beneficial for developing physical-informed extreme value methods.

Future directions based on the analysis tools developed here could enhance understanding of the interplay between physical processes and extreme statistics by including temperature information, and by exploiting other atmospheric variables also described in CPM. Further development of this research could also elucidate variations among ensemble members.

Data Availability Statement

The hourly precipitation data of the CORDEX-FPS on Convection CPM ensemble are in the process of becoming available through the ESGF data nodes. The codes used for the statistical model are freely available at https://doi.org/10.5281/zenodo.11934843 (Marra, 2024), and the codes for the tail test are freely available at https://doi.org/10.5281/zenodo.7234708 (Marra, 2022).

Acknowledgments
We acknowledge the WCRP-CORDEX-FPS on Convective phenomena at high resolution over Europe and the Mediterranean (FPSCONV-ALP-3). This work was supported by CARIPARO Foundation through the ExcellenceGrant 2021 to the "Resilience" Project. GF acknowledges the project "Dipartimento di Eccellenza 2023–2027", funded by the Italian Ministry of Education, University and Research at IUSS Pavia. ED, MB, and MM were supported within the RETURN Extended Partnership and received funding from the European Union Next-GenerationEU (National Recovery and Resilience Plan – NRRP, Mission 4, Component 2, Investment 1.3—D.D. 1243 2/8/2022, PE0000005). FM and MM were supported by the INTENSE project (raINfall exTremEs and their impacts: from the local to the National ScalE) funded by the European Union - Next Generation EU in the framework of PRIN (Progetti di ricerca di Rilevante Interesse Nazionale) programme (Grant 2022ZC2522). We thank the research data exchange infrastructure and services provided by the Jülich Supercomputing Centre, Germany, as part of the Helmholtz Data Federation initiative. For the contribution from Research Centre Jülich, the authors gratefully acknowledge computing time on the supercomputer JURECA at Forschungszentrum Jülich. FM was partially supported by the "The Geosciences for Sustainable Development" project (Budget Ministero dell'Università e della Ricerca–Dipartimenti di Eccellenza 2023–2027 C93C23002690001). Open access publishing facilitated by Universita degli Studi di Padova, as part of the Wiley - CRUI-CARE agreement.

References

Adinolfi, M., Raffa, M., Reder, A., & Mercogliano, P. (2021). Evaluation and expected changes of summer precipitation at convection permitting scale with COSMO-CLM over alpine space. *Atmosphere*, *12*(1), 54. https://doi.org/10.3390/atmos12010054

Amponsah, W., Dallan, E., Nikolopoulos, E. I., & Marra, F. (2022). Climatic and topographic controls on rainfall extremes and their temporal changes in data-sparse tropical regions. *Journal of Hydrology*, *612*, 128090. https://doi.org/10.1016/j.jhydrol.2022.128090

Armon, M., Marra, F., Enzel, Y., Rostkier-Edelstein, D., Garfinkel, C. I., Adam, O., et al. (2022). Reduced rainfall in future heavy precipitation events related to contracted rain area despite increased rain rate. *Earth's Future*, *9*(1), e2021EF002397. https://doi.org/10.1029/2021EF002397

Auer, I., Böhm, R., Jurkovic, A., Lipa, W., Orlik, A., Potzmann, R., et al. (2007). HISTALP—Historical instrumental climatological surface time series of the greater alpine region. *International Journal of Climatology*, *27*(1), 17–46. https://doi.org/10.1002/joc.1377

Avanzi, F., De Michele, C., Gabriele, S., Ghezzi, A., & Rosso, R. (2015). Orographic signature on extreme precipitation of short durations. *Journal of Hydrometeorology*, *16*(1), 278–294. https://doi.org/10.1175/JHM-D-14-0063.1

Baldauf, M., Seifert, A., Förstner, J., Majewski, D., Raschendorfer, M., & T. Reinhardt, T. (2011). Operational convective-scale numerical weather prediction with the COSMO model: Description and sensitivities. *Monthly Weather Review*, *139*(12), 3887–3905. https://doi.org/10.1175/MWR-D-10-05013.1

Ban, N., Rajczak, J., Schmidli, J., & Schär, C. (2020). Analysis of Alpine precipitation extremes using generalized extreme value theory in convection-resolving climate simulations. *Climate Dynamics*, *55*(1–2), 61–75. https://doi.org/10.1007/s00382-018-4339-4

Ban, N., Schmidli, J., & Schär, C. (2014). Evaluation of the convection-resolving regional climate modelling approach in decade-long simulations. *Journal of Geophysical Research: Atmospheres*, *119*(13), 7889–7907. https://doi.org/10.1002/2014JD021478

Belušić, D., de Vries, H., Dobler, A., Landgren, O., Lind, P., Lindstedt, D., et al. (2020). HCLIM38: A flexible regional climate model applicable for different climate zones from coarse to convection-permitting scales. *Geoscientific Model Development*, *13*(3), 1311–1333. https://doi.org/10.5194/gmd-13-1311-2020

Berthou, S., Kendon, E. J., Chan, S. C., Ban, N., Leutwyler, D., Schär, C., & Fosser, G. (2020). Pan-European climate at convection-permitting scale: A model intercomparison study. *Climate Dynamics*, *55*(1–2), 35–59. https://doi.org/10.1007/s00382-018-4114-6

Brunetti, M., Lentini, G., Maugeri, M., Nanni, T., Auer, I., Böhm, R., & Schöner, W. (2009). Climate variability and change in the Greater Alpine Region over the last two centuries based on multi-variable analysis. *International Journal of Climatology*, *29*(15), 2197–2225. https://doi.org/10.1002/joc.1857

Caillaud, C., Somot, S., Alias, A., Bernard-Bouissières, I., Fumière, Q., Laurantin, O., et al. (2021). Modelling mediterranean heavy precipitation events at climate scale: An object-oriented evaluation of the CNRM-AROME convection-permitting regional climate model. *Climate Dynamics*, *56*(5–6), 1717–1752. https://doi.org/10.1007/s00382-020-05558-y

Chan, S. C., Kendon, E. J., Berthou, S., Fosser, G., Lewis, E., & Fowler, H. J. (2020). Europe-wide precipitation projections at convection permitting scale with the Unified Model. *Climate Dynamics*, *55*(3–4), 409–428. https://doi.org/10.1007/s00382-020-05192-8

Chan, S. C., Kendon, E. J., Fowler, H. J., Youngman, B. D., Dale, M., & Short, C. (2023). New extreme rainfall projections for improved climate resilience of urban drainage systems. *Clim. Serv.*, *30*, 100375. https://doi.org/10.1016/j.cliser.2023.100375

Coppola, E., Sobolowski, S., Pichelli, E., Raffaele, F., Ahrens, B., Anders, I., et al. (2020). A first-of-its-kind multi-model convection permitting ensemble for investigating convective phenomena over Europe and the Mediterranean. *Climate Dynamics*, *55*(1–2), 3–34. https://doi.org/10.1007/s00382-018-4521-8

Coppola, E., Stocchi, P., Pichelli, E., Torres Alavez, J. A., Glazer, R., Giuliani, G., et al. (2021). Non-hydrostatic RegCM4 (RegCM4-NH): Model description and case studies over multiple domains. *Geoscientific Model Development*, *14*(12), 7705–7723. https://doi.org/10.5194/gmd-14-7705-2021

Dallan, E., Borga, M., Fosser, G., Canale, A., Roghani, B., Marani, M., & Marra, F. (2024). A method to assess and explain changes in sub-daily precipitation return levels from convection-permitting simulations. *Water Resources Research*, *60*(5), e2023WR035969. https://doi.org/10.1029/2023WR035969

Dallan, E., Borga, M., Zaramella, M., & Marra, F. (2022). Enhanced summer convection explains observed trends in extreme subdaily precipitation in the Eastern Italian Alps. *Geophysical Research Letters*, *49*(5), e2021GL096727. https://doi.org/10.1029/2021GL096727

Dallan, E., Marra, F., Fosser, G., Marani, M., Formetta, G., Schär, C., & Borga, M. (2023). How well does a convection-permitting regional climate model represent the reverse orographic effect of extreme hourly precipitation? *Hydrology and Earth System Sciences*, *27*(5), 1133–1149. https://doi.org/10.5194/hess-27-1133-2023

Formetta, G., Marra, F., Dallan, E., Zaramella, M., & Borga, M. (2022). Differential orographic impact on sub-hourly, hourly, and daily extreme precipitation. *Advances in Water Resources*, *149*, 104085. https://doi.org/10.1016/j.advwatres.2021.104085

Fosser, G., Kendon, E. J., Stephenson, D., & Tucker, S. (2020). Convection-permitting models offer promise of more certain extreme rainfall projections. *Geophysical Research Letters*, *47*(13), e2020GL088151. https://doi.org/10.1029/2020GL088151

Fosser, G., Khodayar, S., & Berg, P. (2015). Benefit of convection permitting climate model simulations in the representation of convective precipitation. *Climate Dynamics*, *44*(1–2), 45–60. https://doi.org/10.1007/s00382-014-2242-1

Fosser, G., Tölle, M., Kendon, E. J., Adinolfi, M., Ban, N., Belušić, D., et al. (2024). Convection-permitting climate models offer more certain extreme rainfall projections. *NPJ Climate and atmospheric science*. https://doi.org/10.1038/s41612-024-00600-w

Fowler, H. J., Ali, H., Allan, R. P., Ban, N., Barbero, R., Berg, P., et al. (2021). Towards advancing scientific knowledge of climate change impacts on short-duration rainfall extremes. *Philosophical Transactions of the Royal Society A: Mathematical, Physical & Engineering Sciences*, *379*(2195), 20190542. https://doi.org/10.1098/rsta.2019.0542

Fowler, H. J., Wasko, C., & Prein, A. F. (2021). Intensification of short-duration rainfall extremes and implications for flood risk: Current state of the art and future directions. *Philos. Trans. R. Soc. A*, *379*(2195), 20190541. https://doi.org/10.1098/rsta.2019.0541

Gobiet, A., Kotlarski, S., Beniston, M., Heinrich, G., Rajczak, J., & Stoffel, M. (2014). 21st century climate change in the European Alps—A review sci. *Total Environ*, *493*(2014), 1138–1151. https://doi.org/10.1016/j.scitotenv.2013.07.050

Hock, R., Bliss, A., Marzeion, B., Giesen, R. H., Hirabayashi, Y., Huss, M., et al. (2019). GlacierMIP – a model intercompari-son of global-scale glacier mass-balance models and projections. *Journal of Glaciology*, *65*(251), 453–467. https://doi.org/10.1017/jog.2019.22

Hosseini, S. R., Scaioni, M., & Marani, M. (2020). Extreme Atlantic hurricane probability of occurrence through the metastatistical extreme value distribution. *Geophysical Research Letters*, *47*(1), 2019GL086138. https://doi.org/10.1029/2019GL086138

Intergovernmental Panel on Climate Change (IPCC). (2023). In V. Masson-Delmotte, P. Zhai, A. Pirani, S. L. Connors, C. Péan, et al. (Eds.), *Climate change 2021: The physical science basis. Contribution of working group I to the sixth assessment report of the intergovernmental panel on climate change*. Cambridge University Press. https://doi.org/10.1017/9781009157896

Kendon, E. J., Ban, N., Roberts, N. M., Fowler, H. J., Roberts, M. J., Chan, S. C., et al. (2017). Do convection-permitting regional climate models improve projections of future precipitation change? *Bulletin of the American Meteorological Society*, *98*(1), 79–93. https://doi.org/10.1175/BAMS-D-15-0004.1

Kendon, E. J., Fischer, E. M., & Short, C. J. (2023). Variability conceals emerging trend in 100yr projections of UK local hourly rainfall extremes. *Nature Communications*, *14*(1), 1133. https://doi.org/10.1038/s41467-023-36499-9

Keuler, K., Radtke, K., Kotlarski, S., & Lüthi, D. (2016). Regional climate change over Europe in COSMO-CLM: Influence of emission scenario and driving global model. *Meteorologische Zeitschrift*, *25*(2), 121–136. https://doi.org/10.1127/metz/2016/0662

Leutwyler, D., Fuhrer, O., Lapillonne, X., Lüthi, D., & Schär, C. (2016). Towards European-scale convection-resolving climate simulations with GPUs: A study with COSMO 4.19. *Geoscientific Model Development*, *9*, 3393–3412. https://doi.org/10.5194/gmd-9-3393-2016

Leutwyler, D., Lüthi, D., Ban, N., Fuhrer, O., & Schär, C. (2017). Evaluation of the convection-resolving climate modeling approach on continental scales. *Journal of Geophysical Research: Atmospheres*, *122*(10), 5237–5258. https://doi.org/10.1002/2016jd026013

Libertino, A., Ganora, D., & Claps, P. (2019). Evidence for increasing rainfall extremes remains elusive at large spatial scales: The case of Italy. *Geophysical Research Letters*, *46*(13), 7437–7446. https://doi.org/10.1029/2019GL083371

Lu, J., Vecchi, G. A., & Reichler, T. (2007). Expansion of the Hadley cell under global warming. *Geophysical Research Letters*, *34*(6), L06805. https://doi.org/10.1029/2006GL028443

Marani, M., & Ignaccolo, M. (2015). A metastatistical approach to rainfall extremes. *Advances in Water Resources*, *79*, 121–126. https://doi.org/10.1016/j.advwatres.2015.03.001

Marani, M., & Zorzetto, E. (2019). Doubly stochastic distributions of extreme events. *arXiv 2019*, arXiv:1902.09862.

Marra, F. (2022). A test for the hypothesis: Block maxima are samples from a parent distribution with Weibull tail. (Version v1). [software]. *Zenodo*. https://doi.org/10.5281/zenodo.7234708

Marra, F. (2024). A unified framework for extreme sub-daily precipitation frequency analyses based on ordinary events - Data and codes - v1.1 (1.2) [data and software]. *Zenodo*. https://doi.org/10.5281/zenodo.11934843

Marra, F., Amponsah, W., & Papalexiou, S. M. (2023). Non-asymptotic Weibull tails explain the statistics of extreme daily precipitation. *Advances in Water Resources*, *173*, 104388. https://doi.org/10.1016/j.advwatres.2023.104388

Marra, F., Borga, M., & Morin, E. (2020). A unified framework for extreme subdaily precipitation frequency analyses based on ordinary events. *Geophysical Research Letters*, *47*(18), e2020GL090209. https://doi.org/10.1029/2020gl090209

Marra, F., Koukoula, M., Canale, A., & Peleg, N. (2024). Predicting extreme sub-hourly precipitation intensification based on temperature shifts. *Hydrology and Earth System Sciences*, *28*(2), 375–389. https://doi.org/10.5194/hess-28-375-2024

Marra, F., Zoccatelli, D., Armon, M., & Morin, E. (2019). A simplified MEV formulation to model extremes emerging from multiple nonstationary underlying processes. *Advances in Water Resources*, *127*, 280–290. https://doi.org/10.1016/j.advwatres.2019.04.002

Martel, J. L., Brissette, F. P., Lucas-picher, P., Troin, M., & Arsenault, R. (2021). Climate change and rainfall intensity – Duration – frequency curves: Overview of science and guidelines for adaptation. *Journal of Hydrologic Engineering*, *26*(10), 1–18. https://doi.org/10.1061/(ASCE)HE.1943-5584.0002122

Miniussi, A., Marani, M., & G Villarini, G. (2020). Metastatistical extreme value distribution applied to floods across the continental United States. *Advances in Water Resources*, *136*, 103498. https://doi.org/10.1016/j.advwatres.2019.103498

Miniussi, A., Villarini, G., & Marani, M. (2020). Analyses through the metastatistical extreme value distribution identify contributions of tropical cyclones to rainfall extremes in the eastern United States. *Geophysical Research Letters*, *47*(7), e2020GL087238. https://doi.org/10.1029/2020gl087238

Müller, S. K., Pichelli, E., Coppola, E., Berthou, S., Brienen, S., Caillaud, C., et al. (2024). The climate change response of alpine-mediterranean heavy precipitation events. *Climate Dynamics*, *62*(1), 165–186. https://doi.org/10.1007/s00382-023-06901-9

Nabat, P., Somot, S., Cassou, C., Mallet, M., Michou, M., Bouniol, D., et al. (2020). Modulation of radiative aerosols effects by atmospheric circulation over the Euro-Mediterranean region. *Atmospheric Chemistry and Physics*, *20*(14), 8315–8349. https://doi.org/10.5194/acp-20-8315-2020

Noël, B., van de Berg, W. J., van Meijgaard, E., Kuipers Munneke, P., van de Wal, R. S. W., & van den Broeke, M. R. (2015). Evaluation of the updated regional climate model RACMO2.3: Summer snowfall impact on the Greenland ice sheet. *The Cryosphere*, *9*(5), 1831–1844. https://doi.org/10.5194/tc-9-1831-2015

Orr, H. G., Ekström, M., Charlton, M. B., Peat, K. L., & Fowler, H. J. (2021). Using high-resolution climate change information in water management: A decision-makers' perspective. *Philos. Trans. R. Soc. A*, *379*(2195), 20200219. https://doi.org/10.1098/rsta.2020.0219

Papalexiou, S. M. (2022). Rainfall generation revisited: Introducing cosmos-2 s and advancing copula-based intermittent time series modeling. *Water Resources Research*, *58*(6). https://doi.org/10.1029/2021WR031641

Peleg, N., Marra, F., Fatichi, S., Molnar, P., Morin, E., Sharma, A., & Burlando, P. (2018). Intensification of convective rain cells at warmer temperatures observed from high-resolution weather radar data. *Journal of Hydrometeorology*, *19*(4), 715–726. https://doi.org/10.1175/JHM-D-17-0158.1

Pepin, N., Bradley, R. S., Diaz, H. F., Baraër, M., Caceres, E. B., Forsythe, N., et al. (2015). Elevation-dependent warming in mountain regions of the world. *Nature Climate Change*, *5*(5), 424–430. https://doi.org/10.1038/nclimate2563

Pichelli, E., Coppola, E., Sobolowski, S., Ban, N., Giorgi, F., Stocchi, P., et al. (2021). The first multi-model ensemble of regional climate simulations at kilometer-scale resolution part 2: Historical and future simulations of pre-cipitation. *Climate Dynamics*, *56*(11–12), 3581–3602. https://doi.org/10.1007/s00382-021-05657-4

Powers, J. G., Klemp, J. B., Skamarock, W. C., Davis, C. A., Dudhia, J., Gill, D. O., et al. (2017). The weather research and forecasting model: Overview, system efforts, and future directions. *Bulletin of the American Meteorological Society*, *98*(8), 1717–1737. https://doi.org/10.1175/BAMS-D-15-00308.1

Prein, A. F., Langhans, W., Fosser, G., Ferrone, A., Ban, N., Goergen, K., et al. (2015). A review on regional convection-permitting climate modeling: Demonstrations, prospects, and challenges. *Reviews of Geophysics*, *53*(2), 323–361. https://doi.org/10.1002/2014RG000475

Raymond, C. A., McGuire, L. A., Youberg, A. M., Staley, D. M., & Kean, J. W. (2020). Thresholds for post-wildfire debris flows: Insights from the Pinal Fire, Arizona, USA. *Earth Surface Processes and Landforms*, *45*(6), 1349–1360. https://doi.org/10.1002/esp.4805

Reggiani, P., Todini, E., Boyko, O., & Buizza, R. (2021). Assessing uncertainty for decision-making in climate adaptation and risk mitigation. *International Journal of Climatology*, *41*(5), 2891–2912. https://doi.org/10.1002/joc.6996

Rockel, B., Will, A., & Hense, A. (2008). The regional climate model COSMO-CLM (CCLM). *Meteorologische Zeitschrift*, *17*(4), 347–348. https://doi.org/10.1127/0941-2948/2008/0309

Rottler, E., Kormann, C., Francke, T., & Bronstert, A. (2019). Elevation-dependent warming in the Swiss Alps 1981–2017: Features, forcings and feedbacks. *International Journal of Climatology*, *39*(5), 2556–2568. https://doi.org/10.1002/joc.5970

Schaaf, B., & Feser, F. (2018). Is there added value of convection-permitting regional climate model simulations for storms over the German Bight and Northern Germany? *Meteorology Hydrology and Water Management*, *6*(2), 21–37. https://doi.org/10.26491/mhwm/85507

Sørland, S. L., Brogli, R., Pothapakula, P. K., Russo, E., Van de Walle, J., Ahrens, B., et al. (2021). COSMO-CLM regional climate simulations in the coordinated regional climate downscaling experiment (CORDEX) framework: A review. *Geoscientific Model Development*, *14*(8), 5125–5154. https://doi.org/10.5194/gmd-14-5125-2021

Trenberth, K. E., Dai, A., Rasmussen, R. M., & Parsons, D. B. (2003). The changing character of precipitation. *Bulletin America Meteorology Social*, *84*(9), 1205–1218. https://doi.org/10.1175/BAMS-84-9-1205

Wasko, C., Sharma, A., & Westra, S. (2016). Reduced spatial extent of extreme storms at higher temperatures. *Geophysical Research Letters*, *43*(8), 4026–4032. https://doi.org/10.1002/2016GL068509

Wilson, P. S., & Toumi, R. (2005). A fundamental probability distribution for heavy rainfall. *Geophysical Research Letters*, *32*(14), L14812. https://doi.org/10.1029/2005GL022465

Zorzetto, E., Botter, G., & Marani, M. (2016). On the emergence of rainfall extremes from ordinary events. *Geophysical Research Letters*, *43*(15), 8076–8082. https://doi.org/10.1002/2016GL069445

Zorzetto, E., & Marani, M. (2019). Downscaling of rainfall extremes from satellite observations. *Water Resources Research*, *55*(2019), 156–174. https://doi.org/10.1029/2018WR022950

Zorzetto, E., & Marani, M. (2020). Extreme value metastatistical analysis of remotely sensed rainfall in ungauged areas: Spatial downscaling and error modelling. *Advances in Water Resources*, *135*(2020), 103483. https://doi.org/10.1016/j.advwatres.2019.103483